HOKKAIDO UNIVERSITY

Title	Establishment of a mouse model of propylthiouracil‐induced antineutrophil cytoplasmic antibody‐associated vasculitis
Author(s)	Masuda, Sakiko; Uchizawa, Momo; Terasaka, Chihiro et al.
Citation	Animal Models and Experimental Medicine, 9(4), 822-828 https://doi.org/10.1002/ame2.70172
Issue Date	2026-03-09
Doc URL	https://hdl.handle.net/2115/100160
Rights(URL)	https://creativecommons.org/licenses/by-nc/4.0/
Type	journal article
File Information	Anim Models and Exp Med - 2026.pdf

Hokkaido University Collection of Scholarly and Academic Papers : HUSCAP

Check for updates

Received: 8 October 2025 | Revised: 25 January 2026 | Accepted: 5 February 2026

DOI: 10.1002/ame2.70172

SHORT COMMUNICATION

Establishment of a mouse model of propylthiouracil-induced antineutrophil cytoplasmic antibody-associated vasculitis

Sakiko Masuda[1] | Momo Uchizawa[1] | Chihiro Terasaka[1] | Takumi Abe[1] | Tetsuro Nakamura[2] | Yuka Nishibata[1] | Yusho Ueda[3] | Daigo Nakazawa[3] | Utano Tomaru[4] | Akihiro Ishizu[1]

[1]Department of Medical Laboratory Science, Faculty of Health Sciences, Hokkaido University, Sapporo, Japan

[2]Kidswell Bio Corporation, Tokyo, Japan

[3]Department of Rheumatology, Endocrinology, and Nephrology, Faculty of Medicine and Graduate School of Medicine, Hokkaido University, Sapporo, Japan

[4]Department of Surgical Pathology, Hokkaido University Hospital, Sapporo, Japan

Correspondence
Sakiko Masuda, Faculty of Health Sciences, Hokkaido University, Kita-12, Nishi-5, Kita-ku, Sapporo 0600812, Japan.
Email: sakikomasuda@hs.hokudai.ac.jp

Abstract

Antineutrophil cytoplasmic antibody (ANCA)-associated vasculitis (AAV) is a systemic autoimmune disease characterized by small-vessel inflammation and the presence of ANCAs, which primarily target myeloperoxidase (MPO) and proteinase 3. Propylthiouracil (PTU), an antithyroid drug, is known as a causative drug of MPO-AAV. PTU induces the formation of DNase I-resistant neutrophil extracellular traps (NETs), which act as autoantigen sources and trigger the production of MPO-ANCAs. Although a rat model of PTU-induced AAV has been established, previous attempts to develop a corresponding mouse model have failed to replicate its histopathological features. In this study, we developed a novel murine model of PTU-induced AAV by enhancing neutrophil recruitment through intraperitoneal injection of thioglycolate, followed by intraperitoneal administration of phorbol 12-myristate 13-acetate and PTU to induce DNase I-resistant NETs. Freund's complete adjuvant was coadministered intradermally to amplify the immune response. This protocol resulted in abundant NET deposition in peritoneal tissues, elevated MPO-ANCA levels, and the development of pauci-immune glomerular lesions that closely resembled those observed in human AAV. Furthermore, a modified enzyme-linked immunosorbent assay (ELISA) reliably quantified murine MPO-ANCA levels. Thus, we established a novel murine model of PTU-induced AAV that recapitulates both the serological and histopathological features of the human disease. This model provides a valuable platform for investigating disease mechanisms, including NETs- and ANCA-mediated AAV pathogenesis.

KEYWORDS
ANCA-associated vasculitis (AAV), glomerulonephritis, mouse model, neutrophil extracellular traps (NETs), propylthiouracil (PTU)

1 | INTRODUCTION

Antineutrophil cytoplasmic antibody (ANCA)-associated vasculitis (AAV) is a systemic small-vessel vasculitis characterized by the presence of ANCAs targeting neutrophil cytoplasmic antigens, such as myeloperoxidase (MPO) and proteinase 3 (PR3). These autoantibodies contribute to the pathogenesis of AAV by activating neutrophils, leading to the release of reactive oxygen species

This is an open access article under the terms of the Creative Commons Attribution-NonCommercial License, which permits use, distribution and reproduction in any medium, provided the original work is properly cited and is not used for commercial purposes.
© 2026 The Author(s). *Animal Models and Experimental Medicine* published by John Wiley & Sons Australia, Ltd on behalf of The Chinese Association for Laboratory Animal Sciences.

(ROS) and neutrophil extracellular traps (NETs), which, in turn, damage vascular endothelial cells and promote inflammation.[1]

NETs are composed of DNA and bactericidal proteins such as MPO and neutrophil elastase and play a dual role in both host defense and autoimmunity.[2] Although essential for pathogen clearance, excessive or persistent NETs have been implicated in autoimmune diseases, including AAV. Under physiological conditions, NETs are degraded by the endogenous enzyme DNase I to limit NET-mediated damage.[3] However, DNase I-resistant NETs have been observed in patients with AAV and are thought to contribute to ANCA production and tissue injury.[4]

Certain drugs, including antithyroid drugs—particularly propylthiouracil (PTU)—can induce AAV.[5] Approximately 10%–30% of patients treated with PTU develop ANCA positivity, and a subset of these patients develop AAV. PTU induces the formation of morphologically abnormal and DNase I-resistant NETs that act as autoantigen sources, thereby triggering MPO-ANCA production.[6] A rat model of PTU-induced AAV has demonstrated the pathogenic role of these NETs.[6] However, rat models have intrinsic limitations, most notably the restricted availability of genetic tools compared to mice, which limits detailed mechanistic studies. Previous attempts to overcome these limitations by establishing a corresponding mouse model have failed to reproduce the characteristic histopathological features of AAV, despite the induction of MPO-ANCA production.[7]

A major limitation of previous mouse models was the inconsistent formation of DNase I-resistant NETs, partly attributable to variability in PTU intake when administered via drinking water, and the drug's short half-life (1–2 h). Additionally, the timing of PTU and phorbol 12-myristate 13-acetate (PMA) administration was not optimized to support NET formation. To address these issues, we developed a protocol involving thioglycolate-induced peritonitis to recruit neutrophils, followed by intraperitoneal administration of PMA and PTU at a defined time point. Freund's complete adjuvant (FCA) was also used to enhance the immune response, and the treatment was repeated weekly to sustain NET formation.

In this study, we aimed to establish a mouse model of PTU-induced AAV that recapitulates both the serological and histopathological features of the disease, with a particular focus on the formation of DNase I-resistant NETs.

2 | MATERIALS AND METHODS

2.1 | Establishment of a PTU-induced AAV mouse model

Seventeen-week-old female BALB/c mice were randomly assigned to four groups ($n = 3$ per group): PMA group, PMA+PTU group, PMA+FCA group, and PMA+PTU+FCA group. To induce sterile peritonitis and recruit neutrophils, each mouse received an intraperitoneal injection of 3% thioglycolate. Neutrophil infiltration into the peritoneal cavity peaks approximately 4 h after injection,[8] at which time PMA (20 nmol/L, Sigma-Aldrich, St. Louis, MO, USA) and PTU (20 μmol/L, Sigma-Aldrich) were administered intraperitoneally to promote DNase I-resistant NET formation. FCA was injected intradermally to enhance the immune response. These treatments were repeated weekly at days 0, 7, 14, and 21 (Figure S1).

On day 28, blood samples were collected via tail vein incision for serological analysis. Plasma was separated from heparinized blood and stored at −80°C until use. All mice were anesthetized with isoflurane and euthanized by cervical dislocation on day 28. Systemic organs were harvested and fixed in formalin for histopathological evaluation. In addition, one kidney from each mouse was snap-frozen for immunofluorescence staining to assess immunoglobulin G (IgG) deposition.

2.2 | Immunofluorescent staining for NETs

To evaluate NET formation in the peritoneal cavity, peritoneal tissue adjacent to the pancreas and spleen was harvested, corresponding to the mesothelial cell layers surrounding these organs. Paraffin-embedded sections were subjected to immunofluorescence staining for NET markers. Antigen retrieval was performed by heating tissue sections at 121°C for 20 min in Tris-EDTA buffer (pH 9.0). After blocking with Protein Block Serum-Free Solution (Dako, Glostrup, Denmark) for 10 min, the sections were incubated overnight at 4°C with goat antihuman MPO antibody (1:100; R&D Systems, Minneapolis, MN, USA). After washing, a rabbit anticitrullinated histone H3 (Cit-H3) antibody (1:400; Abcam, Cambridge, UK) was applied for 60 min at room temperature. Alexa Fluor 488-conjugated donkey antigoat IgG antibody (1:500; Abcam) and Alexa Fluor 594-conjugated antirabbit IgG antibody (1:500; Abcam) were then added for 60 min at room temperature in the dark. Autofluorescence was suppressed using Vector TrueVIEW (Vector Laboratories, Newark, CA, USA), and sections were mounted with VECTASHIELD mounting medium containing 4′,6-diamidino-2-phenylindole (DAPI; Vector Laboratories) before observation under a fluorescence microscope. Owing to the difficulty in tissue collection, quantitative assessment of NET deposition across the entire peritoneal cavity was not feasible, which is a limitation of the study. Nevertheless, all available peritoneal tissue within each histological section was evaluated, and a semiquantitative analysis was performed by counting NET-positive sites in the peritoneal tissue.

2.3 | Measurement of mouse MPO-ANCA

Mouse MPO-ANCA levels were measured using a commercial enzyme-linked immunosorbent assay (ELISA) kit (MPO-ANCA ELISA Kit, #CSB-E08676m, Cusabio, Houston, TX, USA). Initially, measurements were performed according to the manufacturer's instructions. Briefly, standards or plasma samples were sequentially incubated with biotin-conjugated MPO, horseradish peroxidase (HRP)-conjugated avidin, and 3,3′,5,5′-tetramethylbenzidine substrate, with appropriate washing steps between each incubation. The enzymatic reaction was terminated using a stop solution, and absorbance was measured at 450 nm using a Varioskan LUX

25762095, 0, Downloaded from https://onlinelibrary.wiley.com/doi/10.1002/ame2.70172 by Sakiko Masuda - Hokkaido University , Wiley Online Library on [09/03/2026]. See the Terms and Conditions (https://onlinelibrary.wiley.com/terms-and-conditions) on Wiley Online Library for rules of use; OA articles are governed by the applicable Creative Commons License

Multimode Microplate Reader (Thermo Fisher Scientific, Waltham, MA, USA).

To improve detection sensitivity, the protocol was modified by introducing a blocking step using 3% skim milk in phosphate-buffered saline (PBS) containing 0.05% Tween-20 for 1 h at room temperature. Additionally, the biotin-conjugated MPO and HRP-conjugated avidin steps were replaced with HRP-conjugated antimouse IgG antibodies (polyclonal; 1:5000 dilution; SeraCare, Milford, MA, USA) and incubated for 1 h at 37°C. Absorbance was measured at 450 nm. Plasma from untreated 14-week-old BALB/c mice was used as a negative control, and plasma from spontaneous crescentic-glomerulonephritis-forming/Kinjoh (SCG/Kj) mice (6–14 weeks old), which develop crescentic glomerulonephritis and systemic vasculitis with ANCA production,[9,10] was used as a positive control.

2.4 | Histopathological analysis of the kidneys

Paraffin-embedded kidney tissues were sectioned at 2 or 4 μm thickness for histopathological analysis. Sections were stained with hematoxylin and eosin (HE), periodic acid–Schiff (PAS), and periodic acid–methenamine silver (PAM). All glomeruli present in each section were evaluated. Glomeruli were classified as affected if they showed necrosis, crescent formation, or extracapillary proliferative or exudative lesions. Crescent formation was defined as the presence of more than three layers of cells along the Bowman capsule. Extracapillary proliferative lesions were identified as abnormal cellular proliferation located outside the glomerular capillary tuft but within the Bowman capsule. Glomerular necrosis was characterized by the absence of viable nuclei and disruption of the glomerular architecture. The glomerular lesion rate was calculated as the percentage of affected glomeruli relative to the total number examined.

2.5 | Immunofluorescence staining for IgG

Frozen kidney tissues were sectioned at 6 μm thickness and fixed in cold acetone for 5 min. After blocking with Protein Block Serum-Free solution for 10 min, the sections were incubated in the dark at room temperature for 60 min with Alexa Fluor 488-conjugated goat antimouse IgG antibody (1:500 dilution; Abcam). Slides were then mounted with VECTASHIELD mounting medium containing DAPI and examined using a fluorescence microscope.

2.6 | Statistical analysis

Statistical analyses were performed using BellCurve for Excel (Social Survey Research Information Co., Ltd., Tokyo, Japan). One-way analysis of variance (ANOVA) was used for parametric comparisons among multiple groups, followed by Dunnett's post-hoc test to compare each group with the control. Student's *t*-test was applied for parametric comparisons between two groups. A p-value <0.05 was considered statistically significant.

3 | RESULTS

3.1 | DNase I-resistant NET deposition in peritoneal tissues

DNase I-resistant NETs, which play a central role in ANCA production, were induced in the peritoneal cavity by administering 3% thioglycolate, followed by treatment with PMA and PTU. NET deposition in peritoneal tissues was then evaluated. Abundant NETs were observed in mice treated with PMA+PTU+FCA, as demonstrated by the colocalization of the NET markers Cit-H3, MPO, and DNA, with a significantly greater number of NET-positive sites than in any of the three control groups (Figure 1A,B).

3.2 | Elevated MPO-ANCA levels in a newly established mouse model of PTU-induced AAV

To establish a reliable method for detecting murine MPO-ANCA, we first evaluated a commercially available ELISA kit using plasma from SCG/Kj mice as a positive control. Although the standard protocol yielded a valid calibration curve, MPO-ANCA levels in SCG/Kj mouse plasma remained below the detection threshold (Figure S2A). We therefore modified the protocol as described in the Materials and Methods section. The revised protocol produced high absorbance values in SCG/Kj mouse plasma, with age-dependent increases, whereas BALB/c mouse plasma (negative control) showed minimal reactivity (Figure S2B,C). A schematic overview of the modified ELISA is shown in Figure S2D. Using this optimized protocol, we detected elevated MPO-ANCA levels in the PMA+PTU+FCA-treated mice (Figure 1C).

3.3 | Development of glomerular lesions in the mouse model of PTU-induced AAV

Histological analysis of kidney tissues was performed to assess glomerular injury. Representative glomerular histopathology showed focal abnormalities, predominantly extracapillary proliferation, together with exudative changes, necrosis, and crescent formation in the PMA+PTU+FCA-treated group, whereas control groups appeared normal (Figure 1D,E). PAS-positive staining was observed in necrotic lesions of the glomeruli. To distinguish these lesions from immune complex-mediated glomerular injury, IgG deposition was evaluated (Figure 1F). For this purpose, SCG/Kj mice, which possess the *lpr* mutation and display a lupus phenotype, were used as a positive control. These mice exhibited strong glomerular IgG deposition. In contrast, PMA+PTU+FCA-treated

25762095, 0, Downloaded from https://onlinelibrary.wiley.com/doi/10.1002/ame2.70172 by Sakiko Masuda - Hokkaido University , Wiley Online Library on [09/03/2026]. See the Terms and Conditions (https://onlinelibrary.wiley.com/terms-and-conditions) on Wiley Online Library for rules of use; OA articles are governed by the applicable Creative Commons License

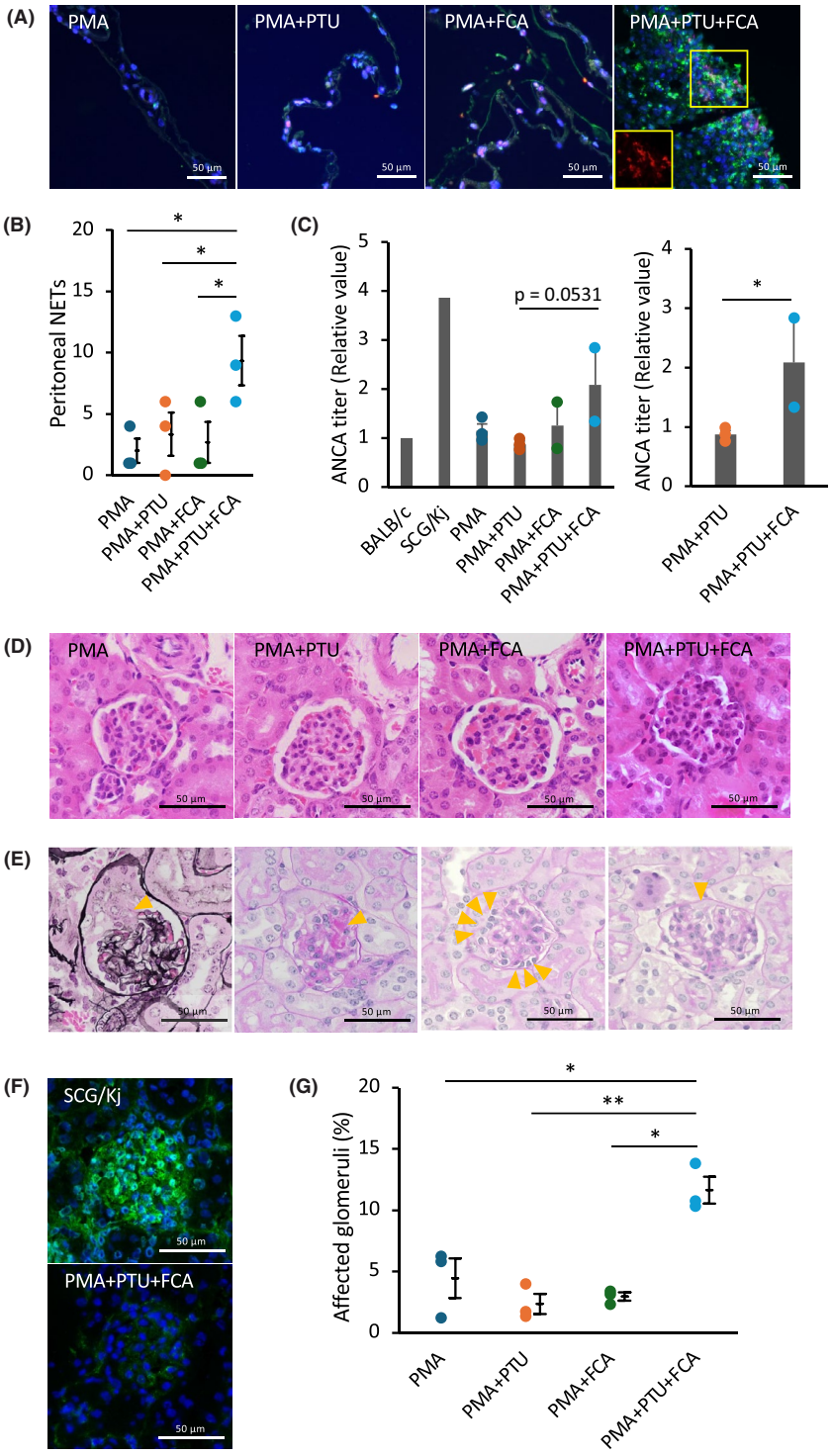


FIGURE 1 Pathological and immunological features of the propylthiouracil (PTU)-induced antineutrophil cytoplasmic antibody (ANCA)-associated vasculitis (AAV) mouse model. (A) Immunofluorescence detection of DNase I-resistant neutrophil extracellular traps (NETs) in peritoneal tissues. Red: Citrullinated histone H3 (Cit-H3, a marker of NET formation); green: Myeloperoxidase (MPO, a neutrophil enzyme); blue: DNA (DAPI staining). Scale bar: 50 μm. Inset: Higher magnification of the boxed area showing Cit-H3 staining. (B) The number of NET-positive sites in peritoneal tissue. $^{*}p < 0.05$. (C) Plasma MPO-ANCA levels on day 28. $^{*}p < 0.05$. In the PMA+FCA-treated and PMA+PTU+FCA-treated groups, one mouse in each group died during anesthesia at the final sampling. Therefore, blood sufficient for the ANCA assessment could not be obtained. (D) Representative glomerular histopathology in each group based on hematoxylin and eosin (HE) staining. Scale bar: 50 μm. (E) Glomerular lesions in the PMA+PTU+FCA group. From left to right: Crescent formation (periodic acid–methenamine silver [PAM] staining); Necrosis (periodic acid–Schiff [PAS] staining); Extracapillary proliferation (PAS staining); Exudative changes (PAS staining). Scale bar: 50 μm. (F) Immunoglobulin (IgG) deposition in the glomeruli of SCG/Kj mouse (14 weeks olds; positive control) and the PMA+PTU+FCA-treated group. Scale bar: 50 μm. (G) Proportion of affected glomeruli. $^{*}p < 0.05$, $^{**}p < 0.01$.

25762095, 0, Downloaded from https://onlinelibrary.wiley.com/doi/10.1002/ame2.70172 by Sakiko Masuda - Hokkaido University , Wiley Online Library on [09/03/2026]. See the Terms and Conditions (https://onlinelibrary.wiley.com/terms-and-conditions) on Wiley Online Library for rules of use; OA articles are governed by the applicable Creative Commons License

mice showed only weak IgG signals, consistent with the pauci-immune pattern characteristic of human AAV. The frequency of glomerular lesions was significantly higher in the PMA+PTU+FCA group compared to controls (Figure 1G). However, when immunofluorescence staining for NETs was performed on kidney sections, Cit-H3 positivity was not detected in any group (data not shown), suggesting that renal NETs may be transient and difficult to detect histologically in this model.

3.4 | Pathological finding of the lungs and other organs

Pulmonary lesions, including alveolar hemorrhage and granuloma formation, were observed in the FCA-treated groups, including the PMA+FCA-treated and PMA+PTU+FCA-treated groups (Figure S3). These groups also exhibited increased background cellularity in the lung. In contrast, the FCA-nontreated groups, including PMA-treated and PMA+PTU-treated groups, showed normal lung histology. Apart from splenomegaly observed in the FCA-treated groups, no remarkable pathological findings were noted in other organs (data not shown).

4 | DISCUSSION AND CONCLUSION

In this study, we established a novel mouse model of PTU-induced AAV that reproduces both serological and histopathological features of the disease. By enhancing neutrophil recruitment with thioglycolate and promoting DNase I-resistant NET formation through PMA and PTU administration, combined with FCA inoculation, we achieved sustained NET formation and robust autoimmune activation. This protocol led to the production of MPO-ANCA and the development of pauci-immune glomerular lesions, closely resembling the renal pathology observed in human AAV.

Importantly, this model exhibits organ involvement and recapitulates the process by which MPO-ANCA production leads to the onset of vasculitis, similar to human AAV. Thus, it may serve as a valuable platform for investigating disease mechanisms and evaluating therapeutic intervention. Although chronological assessment of ANCA titers was not performed in this study, future work will address this limitation to better characterize the disease progression mechanisms of AAV.

In PTU-induced AAV, multiple autoantibodies, including PR3-ANCA, are not rarely produced in addition to MPO-ANCA.[11,12] In the present study, however, we measured solely MPO-ANCA and did not evaluate other relevant autoantibodies. Assessment of a broader autoantibody profile will further enhance a more comprehensive understanding of drug-induced AAV.

The abundant NETs observed in peritoneal tissues suggest that persistent DNase I-resistant NETs may play a central role in breaking immune tolerance and initiating MPO-ANCA production. This finding aligns with the proposed self-amplifying cascade of AAV, in which MPO-ANCA-mediated neutrophil activation leads to further NET release and endothelial damage.

Interestingly, NETs were not detected in kidney tissues, suggesting that their presence in the kidney may be transient and difficult to capture histologically in this model. This contrasts with human AAV, where NETs have been reported in renal biopsies.[13] In addition, glomerular lesions such as extracapillary proliferative changes, exudative changes, crescent formation, and necrosis were observed, with extracapillary proliferation being the predominant finding in this model. In contrast, crescentic lesions are typically more prominent in human AAV. Kidney injury and renal NET deposition in other AAV models are generally milder than those in human AAV,[14,15] which may reflect differences in immune cell composition and immune responses between species. Future studies incorporating chronological analyses and more sensitive NET detection methods will be necessary to clarify the dynamics of renal NET formation and its contribution to disease progression.

Pulmonary lesions, including alveolar hemorrhage and granulomatous changes, were observed in the PMA+PTU+FCA-treated group, and similar findings were also present in the PMA+FCA-treated group. Because these findings were absent in the PMA-treated or PMA+PTU-treated group, granuloma formation with bleeding may be attributable to the strong innate immune activation induced by FCA.

A recent report has shown that in murine AAV models, granulomas are developed in the lungs when intratracheal lipopolysaccharide (LPS) priming is combined with repeated MPO-ANCA administration,[16] whereas other AAV models, including passive and active models, typically exhibited only diffuse alveolar hemorrhage and necrotizing glomerulonephritis without granulomas.[15] In our model, repeated exposure to antigenic stimulation (PMA/PTU) together with FCA may similarly amplify immune activation, potentially contributing to the development of granulomatous lesions. These findings collectively support the notion that granuloma formation in murine AAV models requires not only strong innate and antigen-driven immune activation but also repeated exposure to such stimuli.

In addition to granulomatous lesions, the FCA-treated groups exhibited increased background cellularity in the lungs, which is consistent with previous reports showing that FCA alone can induce pulmonary inflammation accompanied by inflammatory cell infiltration.[17] However, because an FCA-alone group was not included in this study, we cannot exclude the possibility that PMA influenced on the FCA-associated pathology. Future studies using an alternative adjuvant that does not induce granuloma formation should be considered to better evaluate disease-specific pulmonary pathology.

Compared to previous PTU-induced models and the PMA+PTU-treated group, the PMA+PTU+FCA-treated group induced not only MPO-ANCA production and NET formation but also glomerular lesions. Although FCA, LPS, and pertussis toxin were tested in this study as additional stimuli to enhance AAV phenotype, MPO-ANCA production and glomerular lesions occurred only in the FCA-treated

25762095, 0, Downloaded from https://onlinelibrary.wiley.com/doi/10.1002/ame2.70172 by Sakiko Masuda - Hokkaido University , Wiley Online Library on [09/03/2026]. See the Terms and Conditions (https://onlinelibrary.wiley.com/terms-and-conditions) on Wiley Online Library for rules of use; OA articles are governed by the applicable Creative Commons License

group (data not shown). These findings highlight the critical role of FCA in amplifying the autoimmune response.

To facilitate serological evaluation, we modified a commercially available ELISA kit to enable reliable quantification of murine MPO-ANCA. By replacing the original detection reagent with HRP-conjugated antimouse IgG polyclonal antibodies, we improved assay sensitivity and successfully detected age-dependent elevations of MPO-ANCA in SCG/Kj mouse plasma and in our newly developed model. Although the modified protocol was incompatible with the kit's standard substances—likely owing to species mismatch—this approach offers a practical solution for standardizing MPO-ANCA measurements in murine models.

Several limitations should be acknowledged, highlighting areas for future improvement. The primary limitation of this study is the small sample size, which constrains statistical power and generalizability of our conclusions, as this was a preliminary study. Large cohorts will be required to confirm these findings and strengthen statistical validity. Second, this model primarily reflects renal involvement and does not fully replicate systemic manifestations. Because FCA induces strong local and systemic inflammatory responses—including pulmonary inflammation and granulomatous reactions—the pulmonary lesions observed in our study (alveolar hemorrhage and granuloma formation) cannot be clearly distinguished from FCA-associated pathology. These FCA-induced effects may therefore mask disease-specific pulmonary manifestations. In addition, the use of FCA may not accurately reflect natural disease triggers in humans. Alternative adjuvants should be considered to better evaluate pulmonary pathology. Third, although crescent formation is a hallmark of glomerular injury in human AAV, the predominant lesion observed in this model was extracapillary proliferative change. Finally, although the modified ELISA improves MPO-ANCA detection in mice, further validation is required to ensure reproducibility and compatibility with standardized reagents. Collectively, these limitations underscore the need for future studies to refine the model and enhance its translational relevance.

In conclusion, our PTU-induced AAV mouse model provides a valuable platform for investigating the immunopathogenesis of AAV, particularly the role of NETs in ANCA production and vasculitis development. Future improvements should aim to expand organ involvement, explore alternative immunostimulants, and improve assay standardization to enhance the model's translational relevance.

AUTHOR CONTRIBUTIONS

Sakiko Masuda: Conceptualization; data curation; formal analysis; investigation; methodology; visualization; writing – original draft; writing – review and editing. **Momo Uchizawa:** Formal analysis; investigation; visualization; writing – original draft. **Chihiro Terasaka:** Formal analysis; investigation. **Takumi Abe:** Formal analysis; investigation. **Tetsuro Nakamura:** Investigation. **Yuka Nishibata:** Formal analysis; validation. **Yusho Ueda:** Resources; validation. **Daigo Nakazawa:** Resources; validation. **Utano Tomaru:** Formal analysis; validation. **Akihiro Ishizu:** Conceptualization; formal analysis; methodology; project administration; supervision; validation; writing – review and editing.

ACKNOWLEDGMENTS

The authors have no acknowledgments to declare.

FUNDING INFORMATION

The authors did not receive any support from any organization for this study.

CONFLICT OF INTEREST STATEMENT

The authors declare that they have no competing interests.

DATA AVAILABILITY STATEMENT

All data used and/or analyzed in this study are available from the corresponding author on reasonable request.

ETHICS STATEMENT

All animal experiments were approved by the Animal Experiments Committee of Hokkaido University (permission no. 22-0141) and conducted in accordance with the Guidelines for the Care and Use of Laboratory Animals at Hokkaido University.

ORCID

Sakiko Masuda https://orcid.org/0009-0006-8414-7094
Akihiro Ishizu https://orcid.org/0000-0002-7084-9734

REFERENCES

1. Nakazawa D, Masuda S, Tomaru U, Ishizu A. Pathogenesis and therapeutic interventions for ANCA-associated vasculitis. *Nat Rev Rheumatol*. 2019;15(2):91-101. doi:10.1038/s41584-018-0145-y
2. Brinkmann V, Reichard U, Goosmann C, et al. Neutrophil extracellular traps kill bacteria. *Science*. 2004;303(5663):1532-1535. doi:10.1126/science.1092385
3. Hakkim A, Fürnrohr BG, Amann K, et al. Impairment of neutrophil extracellular trap degradation is associated with lupus nephritis. *Proc Natl Acad Sci USA*. 2010;107(21):9813-9818. doi:10.1073/pnas.0909927107
4. Masuda S, Nonokawa M, Futamata E, et al. Formation and disordered degradation of neutrophil extracellular traps in necrotizing lesions of anti-neutrophil cytoplasmic antibody–associated vasculitis. *Am J Pathol*. 2019;189(4):839-846. doi:10.1016/j.ajpath.2019.01.007
5. Wada N, Mukai M, Kohno M, Notoya A, Ito T, Yoshioka N. Prevalence of serum anti-myeloperoxidase antineutrophil cytoplasmic antibodies (MPO-ANCA) in patients with graves' disease treated with propylthiouracil and thiamazole. *Endocr J*. 2002;49(3):329-334. doi:10.1507/endocrj.49.329
6. Nakazawa D, Tomaru U, Suzuki A, et al. Abnormal conformation and impaired degradation of propylthiouracil-induced neutrophil extracellular traps: implications of disordered neutrophil extracellular traps in a rat model of myeloperoxidase antineutrophil cytoplasmic antibody-associated vasculitis. *Arthritis Rheum*. 2012;64(11):3779-3787. doi:10.1002/art.34619
7. Kusunoki Y, Nakazawa D, Shida H, et al. Peptidylarginine deiminase inhibitor suppresses neutrophil extracellular trap formation and MPO-ANCA production. *Front Immunol*. 2016;7:227. doi:10.3389/fimmu.2016.00227

25762095, 0, Downloaded from https://onlinelibrary.wiley.com/doi/10.1002/ame2.70172 by Sakiko Masuda - Hokkaido University , Wiley Online Library on [09/03/2026]. See the Terms and Conditions (https://onlinelibrary.wiley.com/terms-and-conditions) on Wiley Online Library for rules of use; OA articles are governed by the applicable Creative Commons License

8. Itou T, Collins LV, Thorén FB, Dahlgren C, Karlsson A. Changes in activation states of murine polymorphonuclear leukocytes (PMN) during inflammation: a comparison of bone marrow and peritoneal exudate PMN. *Clin Vaccine Immunol*. 2006;13(5):575-583. doi:10.1128/CVI.13.5.575-583.2006
9. Neumann I, Birk R, Newman M, et al. SCG/Kinjoh mice: a model of ANCA-associated crescentic glomerulonephritis with immune deposits. *Kidney Int*. 2003;64(1):140-148. doi:10.1046/j.1523-1755.2003.00061.x
10. Nagao T, Kusunoki R, Iwamura C, et al. Correlation of interleukin-6 and monocyte chemotactic protein-1 concentrations with crescent formation and myeloperoxidase-specific anti-neutrophil cytoplasmic antibody titer in SCG/Kj mice by treatment with anti-interleukin-6 receptor antibody or mizoribine. *Microbiol Immunol*. 2013;57(9):640-650. doi:10.1111/1348-0421.12080
11. Galante JR, Daruwalla CP, Roberts ISD, Haynes R, Storey BC, Bottomley MJ. An unusual presentation of propylthiouracil-induced anti-MPO and PR3 positive ANCA vasculitis with associated anti-GBM antibodies, IgA nephropathy and an IgG4 interstitial infiltrate: a case report. *BMC Nephrol*. 2020;21(1):295. doi:10.1186/s12882-020-01964-w
12. Morita S, Ueda Y, Eguchi K. Anti-thyroid drug-induced ANCA-associated vasculitis: a case report and review of the literature. *Endocr J*. 2000;47(4):467-470. doi:10.1507/endocrj.47.467
13. Kessenbrock K, Krumbholz M, Schönermarck U, et al. Netting neutrophils in autoimmune small-vessel vasculitis. *Nat Med*. 2009;15(6):623-625. doi:10.1038/nm.1959
14. Nishibata Y, Arai S, Taniguchi M, et al. Cathepsin C inhibition reduces neutrophil serine protease activity and improves activated neutrophil-mediated disorders. *Nat Commun*. 2024;15(1):6519. doi:10.1038/s41467-024-50747-6
15. Shochet L, Holdsworth S, Kitching AR. Animal models of ANCA associated vasculitis. *Front Immunol*. 2020;11:525. doi:10.3389/fimmu.2020.00525
16. Hu P, Xiao H, Alba MA, et al. Myeloperoxidase-ANCA IgG induces different forms of small vessel vasculitis based on type of synergistic immune stimuli. *Kidney Int*. 2024;106(5):870-886. doi:10.1016/j.kint.2024.08.022
17. Schurgers E, Mertens F, Vanoirbeek JAJ, et al. Pulmonary inflammation in mice with collagen-induced arthritis is conditioned by complete Freund's adjuvant and regulated by endogenous IFN-γ. *Eur J Immunol*. 2012;42(12):3223-3234. doi:10.1002/eji.201242573

SUPPORTING INFORMATION

Additional supporting information can be found online in the Supporting Information section at the end of this article.

How to cite this article: Masuda S, Uchizawa M, Terasaka C, et al. Establishment of a mouse model of propylthiouracil-induced antineutrophil cytoplasmic antibody-associated vasculitis. *Anim Models Exp Med*. 2026;00:1-7. doi:10.1002/ame2.70172

25762095, 0, Downloaded from https://onlinelibrary.wiley.com/doi/10.1002/ame2.70172 by Sakiko Masuda - Hokkaido University , Wiley Online Library on [09/03/2026]. See the Terms and Conditions (https://onlinelibrary.wiley.com/terms-and-conditions) on Wiley Online Library for rules of use; OA articles are governed by the applicable Creative Commons License